The Journal of Chemical Physics ARTICLE scitation.org/journal/jcp

Fast-release kinetics of a pH-responsive polymer detected by dynamic contact angles

Cite as: J. Chem. Phys. 158, 144901 (2023); doi: 10.1063/5.0142928
Submitted: 18 January 2023 • Accepted: 21 March 2023 •
Published Online: 11 April 2023

Xiaomei Li,[1] Krisada Auepattana-Aumrung,[2] Hans-Jürgen Butt,[1] Daniel Crespy,[2,a)] and Rüdiger Berger[1,a)]

AFFILIATIONS

[1] Max Planck Institute for Polymer Research, Mainz, Germany
[2] Department of Materials Science and Engineering, School of Molecular Science and Engineering, Vidyasirimedhi Institute of Science and Technology (VISTEC), Rayong 21210, Thailand

Note: This paper is part of the JCP Special Topic on Chemical Physics of Controlled Wettability and Super Surfaces.
[a)]**Authors to whom correspondence should be addressed:** daniel.crespy@vistec.ac.th and berger@mpip-mainz.mpg.de

ABSTRACT

Polymers conjugated with active agents have applications in biomedicine, anticorrosion, and smart agriculture. When the active agent is used as a drug, corrosion inhibitor, or pesticide, it can be released upon a specific stimulus. The efficiency and the sustainability of active agents are determined by the released kinetics. In this work, we study the fast-release kinetics of 8-hydroxyquinoline (8HQ) from a pH-responsive, random copolymer of methyl methacrylate and 8-quinolinyl-sulfide-ethyl acrylate [P(MMA-*co*-HQSEA)] by hydrolysis of the *β*-thiopropionate groups. We used contact angle measurements of sliding drops as an elegant way to characterize the release kinetics. Based on the results gained from ^{1}H nuclear magnetic resonance measurement, fluorescent intensity measurement, and velocity-dependent contact angle measurement, we found that both the hydrolysis rate and polymer conformation affect the release kinetics of 8HQ from a P(MMA-*co*-HQSEA) film. Polymer chains collapse and further suppress the release from the inner layer in acidic conditions, while polymer chains in a stretched condition further facilitate the release from the inner layer. As a result, the cumulative release rate of 8HQ is higher in the basic condition than in the acidic condition.

INTRODUCTION

Polymers conjugated with active agents are already being applied in biomedicine, to prevent corrosion, and in smart agriculture.[1–4] Active agents such as drugs, corrosion inhibitors, and pesticides are released from polymers upon a specific stimulus, depending on the type of cleavable bond, the substituents around the bond, and the affinity to the surrounding medium.[3,5] To unravel and control the release kinetics of active agents from polymers to the environment is vital for the success of their applications. A rapid release provides high availability in the short term, while a slow, long-term release maintains a certain level of the active agent.[6,7] Therefore, understanding the release kinetics at all time scales is essential for further specific applications.

Polymer release kinetics depends on the contact time and contact medium. In the case of active agents released from a free polymer chain in a good solvent by a chemical reaction [Fig. 1(a)], the release kinetics is determined by the reaction rate itself. When multiple free polymer chains form a nanoparticle [Fig. 1(b)], the release from the outer layer of the nanoparticle is mainly affected by the reaction rate, while the release from the inner layer is influenced by the conformation of the polymer chains.[8–11] Polymer chains in a collapsed state prevent liquid from penetrating into the inner layer, which, in turn, suppresses the release from the inner layer. In contrast, polymer chains in a stretched state allow liquid penetration, which facilitates release from the inner layer. The release from a condensed polymer film on a substrate is also affected by the polymer conformation, namely, the collapsed state or the stretched state [Fig. 1(c)]. However, the release kinetics is probably different for polymer films and nanoparticles, given their different geometries. To distinguish the influence of reaction rate and polymer conformation, studying the fast-release kinetics is required.

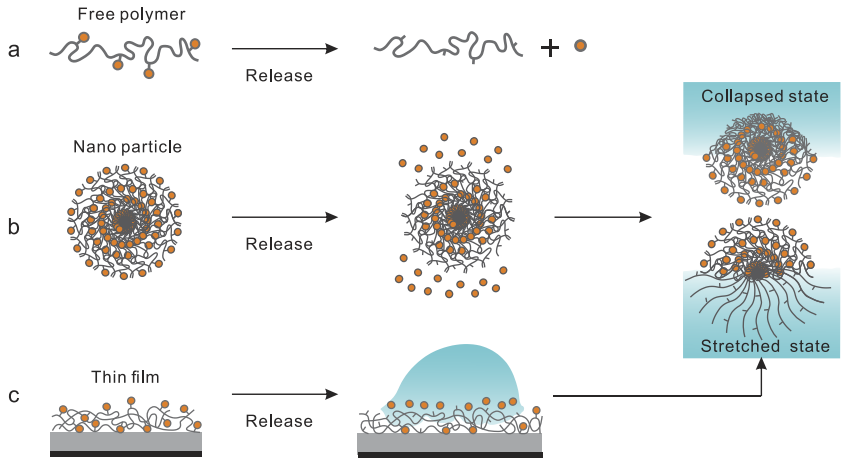

FIG. 1. Schematics showing active agents (orange circles) attached to polymer chains. The active agent is released from a polymer by exposure to a liquid. The polymer forms different states: (a) a free polymer chain, (b) a polymer nanoparticle, and (c) a thin polymer film on a substrate.

To characterize the release kinetics of active agents from polymers, typically ultraviolet–visible spectroscopy, nuclear magnetic resonance spectroscopy (NMR), and high-performance liquid chromatography (HPLC) are applied.[12,13] The latter two techniques require an experimental time for a quantitative analysis of at least a few minutes or even longer. In these cases, a burst release with high errors usually appears in the release profiles, because a large quantity of molecules is released in a very short time. Thus, until now, only very limited knowledge about the release kinetics at shorter time scales is available. Here, we propose to use contact angle measurements directly near the three-phase contact line of sliding drops as a way to characterize the release kinetics.

The relationship between the release kinetics and the dynamic contact angles can be described by the adaptation model proposed by Butt *et al.* in 2018.[14] In the adaptation model, surface adaptation causes a change in the chemical/physical properties of the surfaces. The chemical/physical properties of the surfaces later lead to a change of the interfacial energies and the contact angle. For example, liquid diffusion and polymer reorientation at the interface change the contact angle.[15,16] We assume that the changes in surface energy due to the hydrolysis reaction follow first-order kinetics. Then, the exponentially relaxing interfacial energies are described by

$$\gamma(t) = \gamma^{\infty} + \Delta\gamma e^{-t/\tau}, \tag{1}$$

where τ is the relaxation time correlated with the release, γ^{∞} is the equilibrium interfacial energy, and Δγ is the change in interfacial energy due to surface adaptation. The peripheral length (l) is defined as the width in the contact region, which determines the contact angles. By replacing the time t by the ratio between the peripheral length and the contact-line velocity (v), we can rewrite Eq. (1) as

$$\gamma(t) = \gamma^{\infty} + \Delta\gamma e^{-l/v\tau}. \tag{2}$$

Assuming that Young's model is still valid locally and with the surface energies in Young's model described by Eq. (2), the advancing angle (θ_A) and the receding angle (θ_R) can be quantified by the two equations

$$\cos\theta_A = \cos\theta_A^{\infty} - \frac{\Delta\gamma_{SL}}{\gamma_L^{\infty}} e^{-l/v\tau_{SL}}, \tag{3}$$

$$\cos\theta_R = \cos\theta_R^{\infty} + \frac{\Delta\gamma_S}{\gamma_L^{\infty}} e^{-l/v\tau_S}. \tag{4}$$

Here, θ_A^{∞} and θ_R^{∞} are the static advancing and receding contact angles that are valid for $v \to 0$. The subscripts "S," "L," and "S/L" correspond to the solid/air, liquid/air, and solid/liquid interfaces. Measurements of the dynamic advancing and receding contact angles can be performed, e.g., by tilted plate experiments.[15–17] The relaxation time can be calculated by fitting the measured dynamic contact angles vs velocity with Eqs. (3) or (4). A general unknown parameter is the peripheral length. Here, we assume a peripheral length to be around 10 nm, which is a typical length scale for surface force and surface stress.[14] Generally, multiple adaptation processes can lead to changes in contact angles. To distinguish them, a reference surface is required, to attribute change of surface energy (chemical composition or topography) to hydrolysis of the surface. Then, the adaptation model can be used to fit the experimental data.

In this work, we investigate the release kinetics of active agents in solution and from thin polymer films. We explore the release kinetics of 8-hydroxyquinoline (8HQ) from a pH-reactive, random copolymer of methyl methacrylate (MMA) and 8-quinolinyl-sulfide-ethyl acrylate (HQSEA) [P(MMA-*co*-HQSEA)]. P(MMA-*co*-HQSEA) is a random pH-responsive copolymer, with 8-hydroxyquinoline (8HQ) as the active agent. The 8HQ groups are linked to the polymer chains with β-thiopropionate groups and can be released by a hydrolysis reaction. Due to the electron-withdrawing sulfide on the β-thiopropionate groups, the hydrolysis reaction is sensitive to the presence of acids or bases.[7,18–23] The released 8HQ groups can work as inhibitors for metal corrosion or proteasome; therefore, β-thiopropionate polymers with the active agent of 8-hydroxyquinoline (8HQ) have potential applications in the fields of anticorrosion and biomedicine.[24–26] Thus, P(MMA-*co*-HQSEA) is a representative polymer for studying the release kinetics of active agents.

EXPERIMENTAL SECTION

1. **Materials:** methyl methacrylate (MMA, 99%, Acros Organics) was purified by distillation before use. 8-quinolinyl-sulfide-ethyl acrylate (HQSEA) was synthesized according to a previously reported method.[25] *N*,*N*-Dimethylformamide extra dry (DMF, 99.8%, Acros Organics), 1,1′-azobis (cyclohexanecarbonitrile) (ABCN, 98%, Sigma-Aldrich), diisopropyl ether (99%, Carlo Erba), dichloromethane (DCM, 99.9%, Honeywell), aluminum chloride ($AlCl_3$, 99%, Acros Organics), 1,4-dimethoxybenzene (>99%, Tokyo Chemical Industry), chloroform-d_1 ($CDCl_3$, 99.8%, Cambridge Isotope Laboratories, Inc.), deuterium oxide (D_2O, 99.96%, Cambridge Isotope Laboratories), dimethyl sulfoxide-d_6 (99.9%, Cambridge Isotope Laboratories), hydrochloric acid (HCl, 37%, Carlo Erba), potassium hydroxide (KOH, 85%, Carlo Erba), sodium hydroxide (NaOH, 97%, Carlo Erba), di-sodium tetraborate (99.5%, QReC), boric acid (99.8%, Carlo Erba), monosodium phosphate (98%, Carlo Erba), glacial acetic acid (99.5%, Carlo Erba), pH 3 citric buffer solution (citric/sodium hydroxide/sodium chloride, Fluka), pH 3 phosphate buffer solution (Fisher Chemical), pH 4 buffer solution (citric/sodium hydroxide/sodium chloride, Fluka), pH 5.5 buffer solution (sodium acetate, AmBion), pH 7 buffer solution (Sodium phosphate, Alfa Aesar), pH 8 buffer solution (Sodium phosphate, Alfa Aesar), and pH 10 buffer solution (Borax/sodium hydroxide, Fluka) were used without further purification. Deionized water was used throughout this experimental work.
2. **Polymer synthesis:** HQSEA (1660.45 mg, 5.00 mmol) and MMA (500.60 mg, 5.00 mmol) were dissolved in 6 ml of DMF in a 25-ml, round-bottom flask. After adding ABCN (24.43 mg, 0.1 mmol) as the reaction's initiator, the liquid was bubbled with nitrogen gas for 5 min. The reaction flask was then placed in an oil bath at 80 °C in a nitrogen atmosphere for 20 h. After polymerization and cooling to room temperature, the products were precipitated into 200 ml cold diisopropyl ether. Then, the products were dissolved in 10 ml dichloromethane and re-precipitated in cold diisopropyl ether two more times. Finally, the product was dried under a vacuum.
3. **Preparation of surfaces:** We used pure poly(methyl methacrylate) (PMMA) as a reference surface for the dynamic contact angle measurement. Both PMMA surfaces and P(MMA-*co*-HQSEA) surfaces were prepared by a home-made dip-coating machine at a dipping speed of 90 mm/min from a solution of 1 wt. % PMMA or P(MMA-*co*-HQSEA) in tetrahydrofuran. After coating, the surfaces were dried under vacuum at room temperature for 10 h. The thickness of the polymer film was ≈18 nm, as measured by scanning force microscopy (Fig. S1).
4. **Scanning Force Microscopy (SFM):** The topography and the thickness of the surfaces were measured by SFM (Dimension Icon, Bruker) in the tapping mode (Fig. S2). SFM tips with a nominal spring constant of 26 N/m and a nominal resonance frequency of 300 kHz were utilized (160AC-NA, OPUS).
5. **^{1}H NMR spectroscopy measurements:** ^{1}H NMR spectra of products dissolved in $CDCl_3$, D_2O, and DMSO-d_6 were recorded at room temperature with a 600 MHz Bruker NMR spectrometer. To study the release kinetics of 8HQ, 2.5 mg P(MMA-*co*-HQSEA) and 0.5 mg 1,4-dimethoxybenzene were dissolved in a mixture of 700 μl of DMSO-d_6 with 70 μl of D_2O (neutral condition), 70 μl of 0.5M HCl solution in D_2O (acidic condition) or 70 μl of 0.5M KOH solution in D_2O (basic solution). The different solutions were then transferred to NMR tubes, which were placed in a shaking incubator (NB-205, N-Biotek), at 30 °C, applying a shaking rate of 100 rpm. The solutions in the NMR tubes were then measured by ^{1}H NMR spectroscopy at different time intervals.
5. **Fluorescence spectroscopy measurements:** The fluorescence intensity of 8HQ was measured by fluorescence spectroscopy (Edinburgh Instruments FLS980 spectrometer). We monitored the temporal evolution of the fluorescence intensity of the released 8HQ from P(MMA-*co*-HQSEA) surfaces. The coated glass substrates were immersed in a 15 ml solution at pH 3, in a solution at pH 7, and in a solution at pH 10 in shaking incubators (NB-205, N-Biotek, 30 °C, 100 rpm). At different time intervals, 2 ml of the buffer solution, including released molecules, was removed for measurements and replaced by 2 ml of fresh buffer solution. A solution at pH 3 was prepared by adding 0.3 g of glacial acetic acid to 225 ml of deionized water, followed by the gradual addition of a 1N HCl aqueous solution, to control the pH value. The volume was then adjusted to 500 ml with deionized water. A solution at pH 7 was prepared by adding 0.6 g of monosodium phosphate to 225 ml of deionized water, followed by the gradual addition of a 1N NaOH aqueous solution, to control the pH value. The volume was then adjusted to 500 ml with deionized water. A solution at pH 10 was prepared by adding 3.1 g of boric acid and 2.5 g of di-sodium tetraborate to 225 ml of deionized water, followed by the gradual addition of a 1N NaOH aqueous solution, to control the pH value. The volume was then adjusted to 500 ml with deionized water. To increase the fluorescence, we added 200 μl of 20 mg/ml $AlCl_3$ aqueous solution to the aliquots taken from the release media. The concentration of 8HQ in the released media was then determined from the measured fluorescence intensity (λ_{ex} = 360 nm and λ_{em} = 530 nm). The calibration curves are provided in the supplementary material (Fig. S2). The cumulative release percentage was calculated using[27]

$$C_n = C_{n\_measured} + \frac{A}{V}\sum_{s=1}^{n-1} C_{s\_measured}. \quad (5)$$

Here, C_n is the expected nth sample concentration, $C_{n\_measured}$ is the measured concentration, A is the volume of the withdrawn aliquot, V is the volume of the dissolution medium, $n-1$ is the total volume of all the previously withdrawn samples before measuring the current sample, and $C_{s\_measured}$ is the total concentration of all previously measured samples taken before the current sample was measured.
6. **Dynamic contact angle measurement:** The experimental setup and procedure were described previously.[15,17] Briefly, ≈35 μl drops were deposited onto a tilted surface by a peristaltic pump (MINIPULS 3, Gilson) at a height of 5 mm. The movement of the drop was recorded by a high-speed camera (FASTCAM Mini UX100, Photron) using a 1.0x SilverTL™

Telecentric Lens from the side. The recorded length was around 1 cm. The video was processed by an adapted drop-shape analysis code from MATLAB (open source DSAfM) version 9.5.0.944 444 (R2018b). The contact-line velocity and the contact angles on the advancing and the receding sides were then calculated automatically using a polynomial fit. The average velocity of the advancing and receding contact lines is defined as drop velocity. The drop velocity was varied by changing the tilt angle from 30° to 70°. Pristine samples were used for every measurement at varying tilt angles. All the buffer solutions for the tilted plate setup were bought and used directly. The influence of the different compositions of buffer solutions is investigated by measuring the dynamic contact angles of a citrate buffer solution and of a phosphate solution at pH 3 on the P(MMA-*co*-HQSEA) surfaces—the nearly identical results for the two cases indicate that the influence of the buffer solution composition is low see Fig. S5 of the supplementary material.

RESULTS AND DISCUSSION

To study the release kinetics of 8HQ under different conditions, we synthesized a random P(MMA-*co*-HQSEA) polymer. The molar ratio between methyl methacrylate and 8-quinolinyl-sulfide-ethyl acrylate units in the copolymer was 1:1, as measured by ^{1}H NMR spectroscopy in $CDCl_3$ [Fig. 2(a)].

The release kinetics of 8HQ from P(MMA-*co*-HQSEA) under neutral, acidic, and basic conditions was investigated by monitoring the ^{1}H NMR spectra in the solutions at different time intervals at 25 °C. The release of 8HQ from P(MMA-*co*-HQSEA) was investigated by comparing the signal of aromatic protons in 8HQ with the signal of protons of 1,4-dimethoxybenzene used as an internal standard [Fig. 2(b) and Fig. S2]. Under neutral conditions [green triangles in Fig. 2(c)], we detected no significant signal from 8HQ. Thus, under neutral conditions, 8HQ was not released or the released amount was too low to be detected. In contrast, more than 70% of 8HQ was released in acidic conditions after 480 h [red squares in Fig. 2(c)]. Moreover, all 8HQ had been released from P(MMA-*co*-HQSEA) in basic conditions within 5 min before the first ^{1}H NMR measurement [blue circles in Fig. 2(c)]. Hydrolysis of β-thiopropionate groups under the acidic and basic conditions was, therefore, faster than that under neutral conditions, confirming previous reports.[4,28] However, the release kinetics of 8HQ on a very short time scale (for example, in basic solution) could not be detected by ^{1}H NMR spectroscopy because of the relatively low sensitivity and long measuring time.

To slow down the release kinetics of 8HQ, we used a dense, 18-nm-thick P(MMA-*co*-HQSEA) film on a glass substrate, immersed in solutions with different pH values. 8HQ is a weakly fluorescent molecule due to intramolecular proton transfer from the hydroxyl group to the nitrogen atom in the excited state. However, chelation of metal cations can prevent this transfer, rendering the 8HQ complex highly fluorescent.[25,29,30] For this reason, a measurement of fluorescent intensity is also a normal way to explore the release kinetics of 8HQ after adding 20 mg/ml $AlCl_3$ to the solution. Upon light excitation at 360 nm, the chelated 8HQ displayed a fluorescence emission at 530 nm. The cumulative amount of released 8HQ could be calculated based on the calibration curves see Fig. S3 of the supplementary material.

We measured an increasing fluorescence intensity over time after immersing the film in the basic solution at pH 10 [Fig. 3(a)]. The cumulative release percentages of 8HQ in acidic and basic conditions were 7.5% and 7.8%, respectively, after 72 h of immersion [Fig. 3(b)]. Consistent with the NMR results, the P(MMA-*co*-HQSEA) film in neutral conditions did not display measurable fluorescence. At the early stage of immersion (1–6 h), the release of 8HQ from the coating in the basic condition was faster than that in the acidic condition, also in line with the NMR results. Since the fluorescence intensity of the released 8HQ in the first 1 h after immersing the samples was low, the release kinetics on a time scale of up to 1 h could not be resolved [Fig. 3(a)].

To study the release kinetics of 8HQ on a time scale ≤1 s and to distinguish the influence of hydrolysis rate from that of polymer conformation, we measured the velocity-dependent contact angles of sliding drops on P(MMA-*co*-HQSEA) films. Even on non-adaptive surfaces, the dynamic advancing contact angles increased, while the dynamic receding contact angles decreased, with increasing contact-line velocity. This effect is known and originates from viscous energy dissipation and contact-line friction.[31–33] To exclude the influence of non-adaptive energy dissipation and to consider only the changes in dynamic contact angles by surface adaptation due to the release of 8HQ and the presence of carboxyl acid groups, a non-hydrolyzed PMMA surface was used as a reference. On the PMMA surfaces, the dynamic advancing contact angles increased slightly from 76° to 82°. The dynamic receding contact angles decreased from 60° to 35° at a contact-line velocity of 0.3 m/s for a buffer solution at pH 3 [Fig. 4(a), gray].

The relevant contact time between a sliding drop and a P(MMA-*co*-HQSEA) surface on the advancing side is different from that on the receding side, giving us different time windows during which we could study the release kinetics. On the advancing side of a sliding drop, the relevant time scale is $\tau_{SL} = l/v$. At pH 3, the dynamic advancing contact angle on the P(MMA-*co*-HQSEA) surface was almost constant (~82°) and the same as the dynamic advancing contact angle of the PMMA surface for velocities >2 cm/s [Fig. 4(a), red]. Then, it decreased from 80° to 60° for velocities <2 cm/s. At a velocity U → 0, the static advancing contact angle (θ_a^∞ = 66°) was 10° lower than the one on the PMMA surface (θ_a^∞ = 76°). This result indicates that the copolymer surfaces became more hydrophilic compared to the PMMA surface after contact with an acidic drop. That means that the P(MMA-*co*-HQSEA) surface adapts when it contacts the sliding drop at low velocity. Fitting the velocity-dependent dynamic advancing contact angles to Eq. (3), we obtained the fitting parameter of the peripheral length divided by relaxation time [Fig. 4(b)]. Using 10 nm as the peripheral length, we calculated the relaxation times for drops at pH 3 to be around 3 μs. The relaxation time indicates the time needed to reduce the solid/liquid interfacial energies to 37% of their initial value. Varying the pH value of the sliding drop changes the critical contact-line velocities at which the dynamic advancing contact angles start to increase with velocity [Fig. 4(a) and Fig. S4, circles]. This observation indicates that the relaxation time of surface adaptation for solutions at different pH values varies. The relaxation time increased from around 1 to 5 μs when the pH value increased from 3 to 7, and when pH > 7, it saturated at around 5 μs [Fig. 4(c)]. In the

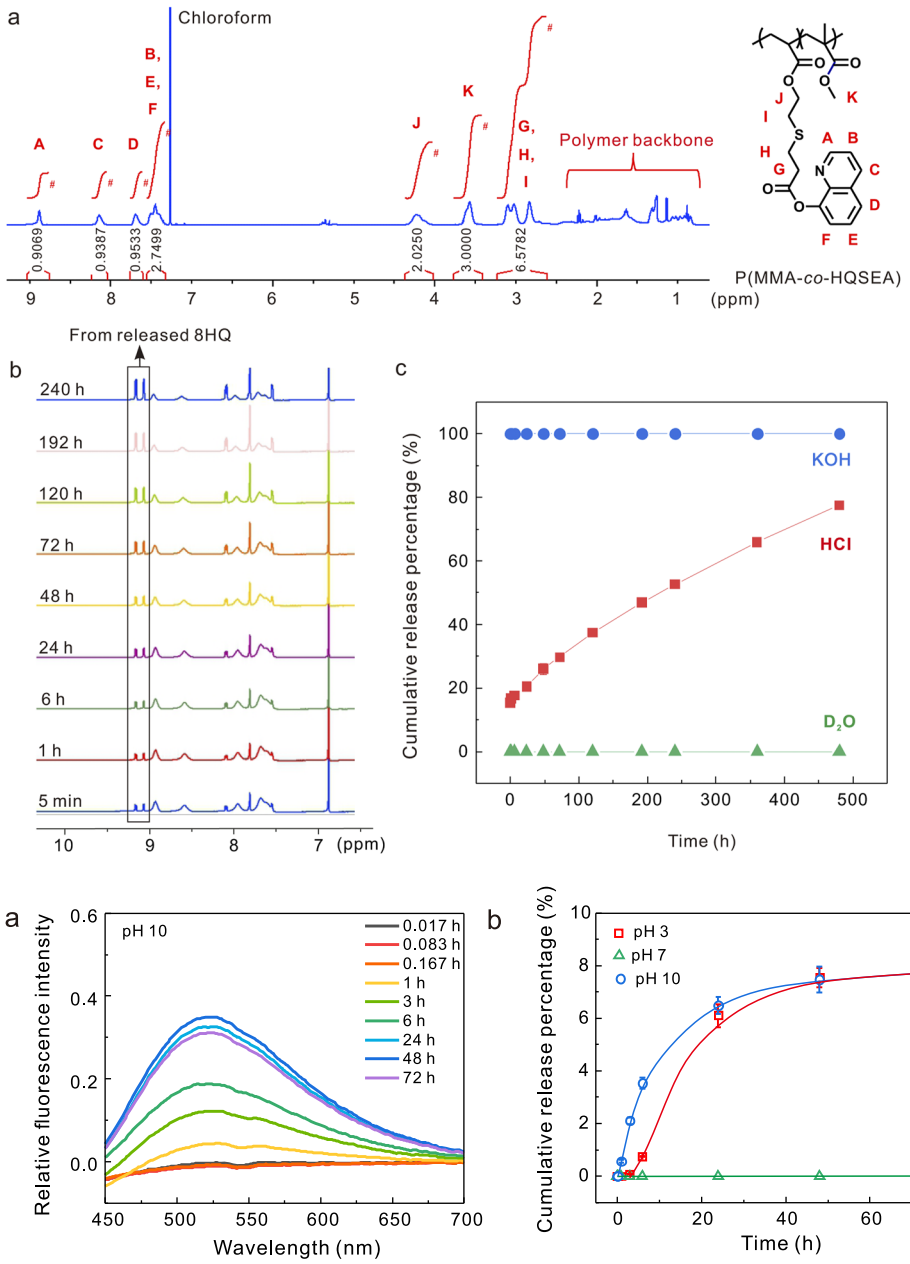

FIG. 2. Representative results of ^{1}H NMR measurements. (a) ^{1}H NMR spectrum of P(MMA-*co*-HQSEA) in $CDCl_3$. (b) Temporal evolution of the ^{1}H NMR spectra of a solution of P(MMA-*co*-HQSEA) in an acidic condition. (c) Temporal evolution of the cumulative release percentage of 8HQ from P(MMA-*co*-HQSEA) in neutral, acidic (pH ≈ 0.3), and basic (pH ≈ 13.7) conditions.

FIG. 3. The results of fluorescence microscopy measurements. (a) The typical change in the fluorescence spectrum of 8HQ over time in the solution at pH 10. (b) Temporal evolution of the release of 8HQ from P(MMA-*co*-HQSEA) solutions at pH 3, pH 7, and pH 10, measured by fluorescence spectroscopy.

literature, the time needed for protonation/deprotonation of the nitrogen atom at the quinolinyl group is microseconds.[34] Thus, one possible explanation for the adaptation of the P(MMA-*co*-HQSEA) surface could be protonation in acidic conditions, which makes the surface hydrophilic. However, the protonation effect does not explain why the P(MMA-*co*-HQSEA) surface also becomes hydrophilic in the basic condition. Based on the above-mentioned ^{1}H NMR measurements, an alternative explanation for the adaptation of the P(MMA-*co*-HQSEA) surface would be hydrolysis of the *β*-thiopropionate group on the advancing side of the drop. Hydrolysis leads to the presence of carboxyl groups after releasing 8HQ, which makes the surface more hydrophilic. In this case, the hydrolysis time would be a few microseconds, which is surprisingly short.

The diffusion coefficient (D) for water in PMMA or in PAA polymer film is around 10^{-12} to 10^{-13} m^2/s.[35,36] The time needed for water to diffuse 10 nm deep (Δz) into a polymer film is ($\tau = \frac{\Delta z^2}{D}$) ≈ 10 ms, which is longer than a few microseconds.[14–16] According to the time scale, hydrolysis would only affect the outer layer of the sample on the advancing side. Lower advancing contact angles [Fig. 4(b)] and shorter relaxation time [Fig. 4(c)] of drops at pH 3 indicate that the hydrolysis reaction would be faster in the acidic solution than in the basic solution (drops at pH 10). The shorter relaxation time is consistent with the hypothesized hydrolysis

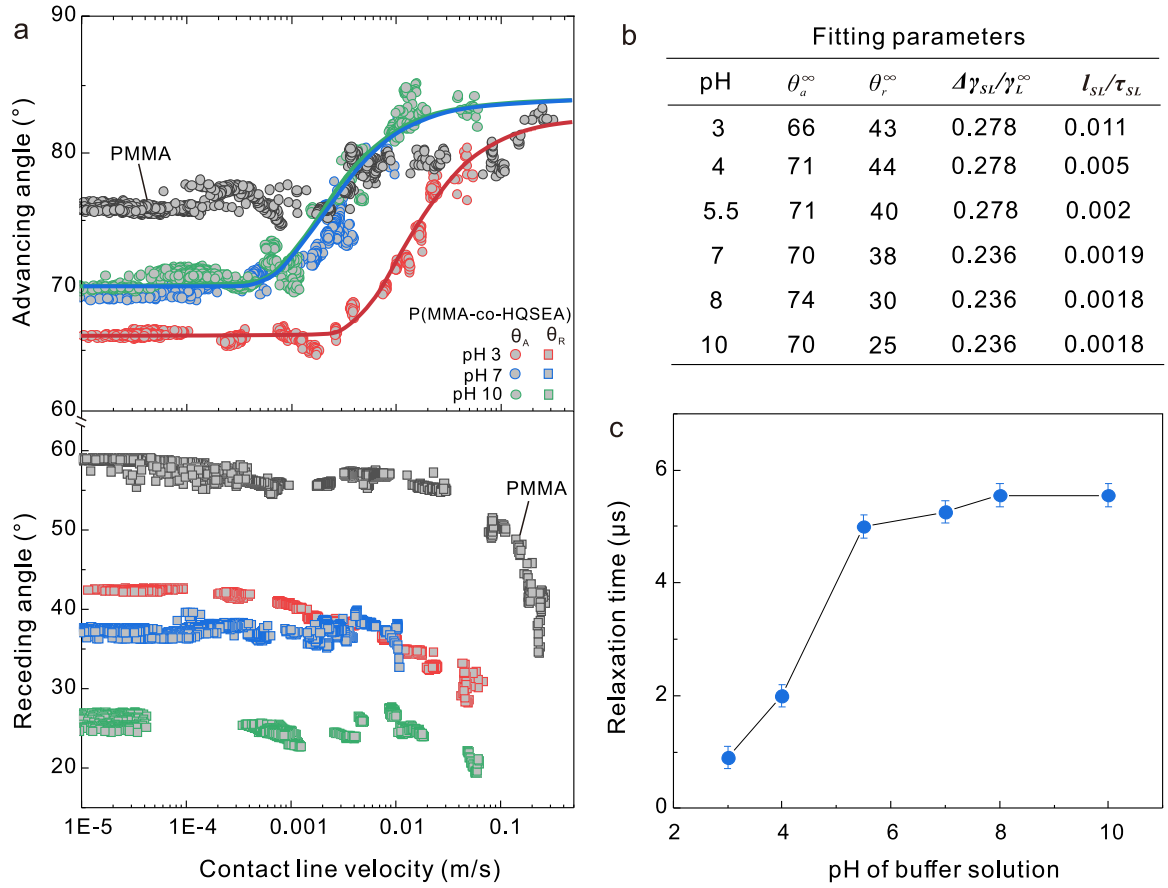

pH	θ_a^∞	θ_r^∞	$\Delta\gamma_{SL}/\gamma_L^\infty$	l_{SL}/τ_{SL}
3	66	43	0.278	0.011
4	71	44	0.278	0.005
5.5	71	40	0.278	0.002
7	70	38	0.236	0.0019
8	74	30	0.236	0.0018
10	70	25	0.236	0.0018

FIG. 4. The results of the dynamic contact angle measurements of pristine samples. Dynamic contact angles were measured for drops with a volume of 35 μl which slid down a tilted plate at different tilt angles. (a) Velocity-dependent contact angles of drops at different pH values, sliding down the P(MMA-*co*-HQSEA) surfaces and inert PMMA surfaces. Circles represent the dynamic advancing angles, while rectangles represent the dynamic receding contact angles. (b) Fitting parameters for the fitting curves are given in Fig. 4(a) and Fig. S4. (c) Evolution of the relaxation time with the pH values of the drops.

mechanism of the β-thiopropionate groups.[4,23] In the acidic solutions, sulfur atoms are protonated, which increases the positive charge on the carbon atom of the ester group and makes the formation of a six-membered ring intermediate easier (Fig. 5). Therefore, the hydrolysis in acidic conditions could be faster than the hydrolysis in basic conditions.

However, our observation and hypothesis that the hydrolysis reaction is faster in acidic solutions seem to contradict the lower cumulative release rate of 8HQ measured by NMR and fluorescent microscopy [Figs. 2(c) and 3(b)]. In fact, the measurements of NMR and fluorescence intensity only reveal the cumulative release rate. In addition to the hydrolysis rate, the cumulative release rate is affected by the polymer conformation. The influence of polymer conformation is visible on the receding side of the drop in our sliding drop experiments on polymer films. Sliding drops have a contact length of around 5 mm. On the receding side, the contact time between a sliding drop and a P(MMA-*co*-HQSEA) surface is in the range 0.05–500 s at a contact line velocity ranging from 0.1 to 10^{-5} m/s. Even the shortest contact time on the receding side of the drop (50 ms) is already longer than the hypothetical hydrolysis reaction time (5 μs) on the advancing side. In addition, 50 ms is long enough to allow water to diffuse deeper into the polymer film. Thus, the 8HQ could be released from the inner layer of the film. After releasing 8HQ from the outer layer, the remaining moiety polyacrylate (PAA) is a kind of polyelectrolyte with *pKa* of 4.5.[37] In the acidic solution with pH < 4.5, the functional group (–COOH) in polymer chains is primarily un-dissociated and protonated. Because of the inter-/intra-molecular H-bonding attraction between fully protonated carboxyl groups, the liquid tends to be excluded from the polymer mesh, leading to a collapsed conformation of the polymer [Figs. 1(b) and 5]. In this case, the 8HQ in the inner layer is protected by the collapsed polymer chains. Release from the inner layer is suppressed. However, in a basic solution with pH ≫ 4.5, the functional group (–COOH) in the polymer chains manifests as a carboxylate anion ($-COO^-$). Because of electrostatic repulsion between neighboring chains and the same chain, the polymer chains show stretched conformation [Figs. 1(b) and 5]. As a result, the liquid penetrates the inner layer and facilitates the release of 8HQ from

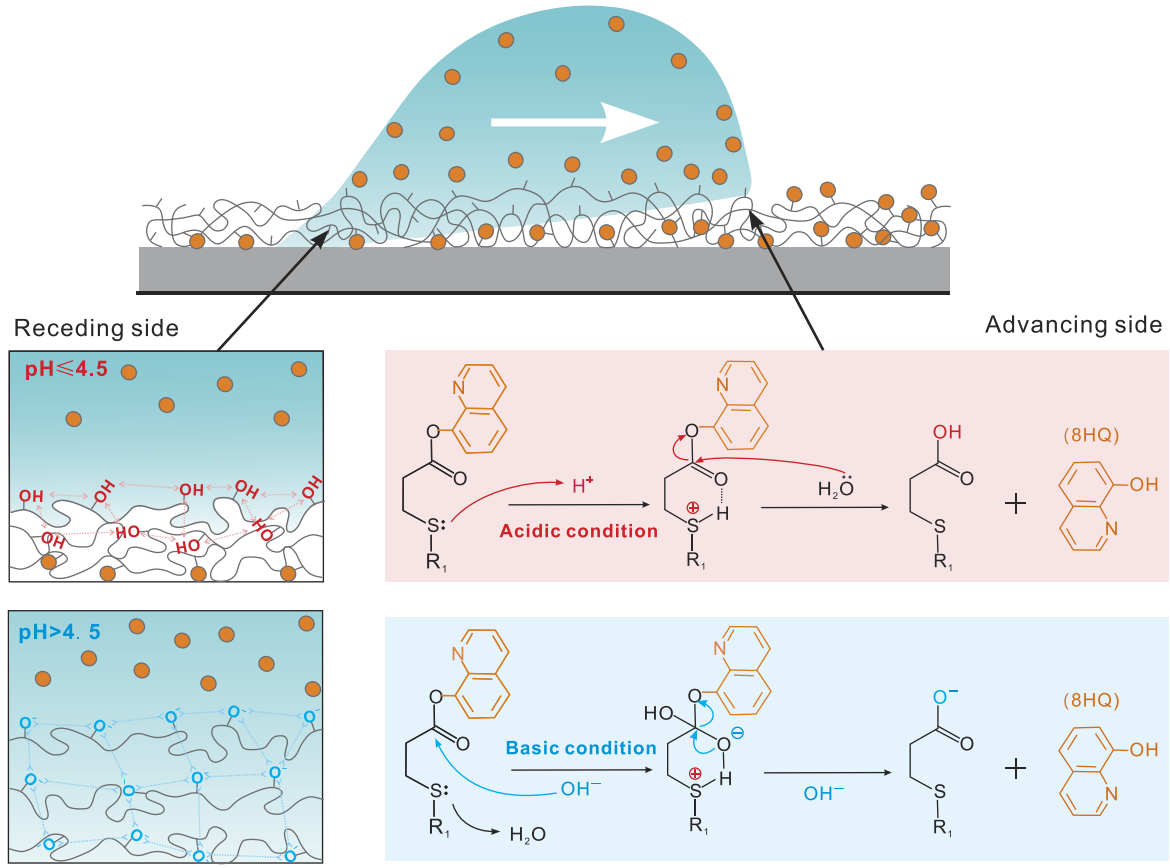

FIG. 5. The schematic of release steps of 8HQ from the P(MMA-*co*-HQSEA) surfaces when the surfaces are in contact with the drops.

the inner layer, leading to a higher cumulative release percentage and lower receding contact angles. In fact, the static receding contact angles of the low-velocity regime (<0.01 m/s) decrease with the increase of pH [Fig. 4(a) and Fig. S4 in the supplementary material, rectangles], in line with above expectations and with the cumulative released percentage measured by NMR and fluorescence microscopy.

CONCLUSIONS

In summary, the release of active agents (8HQ) from pH-responsive P(MMA-*co*-HQSEA) thin films was affected by the hydrolysis rate and polymer conformation. The release kinetics in the outer layer of thin films is dominated by the hydrolysis rate, whereas the release kinetics in the inner layer is influenced by both the hydrolysis rate and polymer conformation. After partially releasing 8HQ from the outer layer, the polymer chains assumed a collapsed state in the acidic condition, while taking on a stretched state in the basic solution. Therefore, the cumulative release rate of 8HQ is higher in the basic solution than in the acidic solution. Using velocity-dependent contact angle measurements, we were able to study the fast-release kinetics at a time scale <1 s, which paves the way to release kinetics at very short time scales.

SUPPLEMENTARY MATERIAL

The supplementary material includes the surface morphology characterization by scanning force microscopy; ^{1}H NMR spectra of P(MMA-*co*-HQSEA) in the acidic, neutral, and basic conditions; calibration curves of 8HQ concentration in solutions of pH 3, pH 7, and pH 10; velocity-dependent dynamic contact angles of drops at pH 4, pH 5.5, and pH 8 on the P(MMA-*co*-HQSEA) surfaces, and velocity-dependent dynamic contact angles of a citrate buffer solution and a phosphate buffer solution at pH 3 on the P(MMA-*co*-HQSEA) surfaces.

ACKNOWLEDGMENTS

This project has received funding from (1) the Priority Program 2171 "Dynamic wetting of flexible, adaptive, and switchable surfaces" (Grant Nos. BU 1556/36 and BE 3286/6-1: X.L., H.-J.B., and R.B.); (2) the European Research Council (ERC) under the

European Union's Horizon 2020 research and innovation program (Grant No. 883631) (H.-J.B.); (3) the NSRF (National Science, Research, and Innovation Fund) via the Program Management Unit for Human Resources & Institutional Development, Research and Innovation (Grant No. B05F640208) (D.C.).

AUTHOR DECLARATIONS

Conflict of Interest

The authors have no conflicts to disclose.

Author contributions

X.L. and K.A.-A. contributed equally to this work. R.B. and D.C. conceived and supervised the project. X.L. and K.A.-A. planned, conducted the experiments, and analyzed the data. All the authors discussed, reviewed, wrote, and approved the manuscript.

Xiaomei Li: Data curation (equal); Investigation (equal); Writing – original draft (equal). **Krisada Auepattana-Aumrung**: Data curation (equal); Investigation (equal); Writing – original draft (equal). **Hans-Jürgen Butt**: Project administration (equal); Writing – review & editing (equal). **Daniel Crespy**: Conceptualization (equal); Writing – review & editing (equal). **Rüdiger Berger**: Conceptualization (lead); Writing – review & editing (equal).

DATA AVAILABILITY

The data that support the findings of this study are available within the article and its supplementary material.

REFERENCES

[1] G. Kocak, C. Tuncer, and V. Bütün, Polym. Chem. **8**, 144 (2017).
[2] N. Dararatana, F. Seidi, and D. Crespy, Polym. Chem. **11**, 4723 (2020).
[3] Y. Xue *et al.*, Chem. Soc. Rev. **50**, 4872 (2021).
[4] F. Seidi, R. Jenjob, and D. Crespy, Chem. Rev. **118**, 3965 (2018).
[5] F. Seidi *et al.*, Chem. Soc. Rev. **51**, 6652 (2022).
[6] P. Phoungtawee *et al.*, ACS Macro Lett. **10**, 365 (2021).
[7] K. Auepattana-Aumrung, T. Phakkeeree, and D. Crespy, Prog. Org. Coat. **163**, 106639 (2022).
[8] O. Azzaroni, A. A. Brown, and W. T. S. Huck, Adv. Mater. **19**, 151 (2007).
[9] F. Zhou and W. T. S. Huck, Chem. Commun. **48**, 5999 – 6001 (2005).
[10] Q. Wei *et al.*, Macromolecules **46**, 9368 (2013).
[11] T. Chen *et al.*, Prog. Polym. Sci. **35**, 94 (2010).
[12] N. Kamaly *et al.*, Chem. Rev. **116**, 2602 (2016).
[13] N. Dararatana *et al.*, Polym. Chem. **11**, 1752 (2020).
[14] H.-J. Butt *et al.*, Langmuir **34**, 11292 (2018).
[15] X. Li *et al.*, Langmuir **37**, 1571 (2021).
[16] X. Li *et al.*, Macromol. Rapid Commun. **43**, 2100733 (2022).
[17] X. Li *et al.*, Nat. Phys. **18**, 713 – 719 (2022).
[18] K. Dan and S. Ghosh, Angew. Chem. **125**, 7441 (2013).
[19] S. Lv *et al.*, J. Controlled Release **194**, 220 (2014).
[20] M. R. Molla *et al.*, Biomacromolecules **15**, 4046 (2014).
[21] P. Pramanik *et al.*, Macromol. Rapid Commun. **37**, 1499 (2016).
[22] B. Klahan, F. Seidi, and D. Crespy, Macromol. Chem. Phys. **219**, 1800392 (2018).
[23] N. Kongkatigumjorn *et al.*, Chem. Mater. **34**, 2842 (2022).
[24] F. Chiter *et al.*, Phys. Chem. Chem. Phys. **17**, 22243 (2015).
[25] N. Dararatana, F. Seidi, and D. Crespy, ACS Appl. Mater. Interfaces **10**, 20876 (2018).
[26] K. Auepattana-Aumrung and D. Crespy, Chem. Eng. J. **452**, 139055 (2023).
[27] I. H. Ali, I. A. Khalil, and I. M. El-Sherbiny, ACS Appl. Mater. Interfaces **8**, 14453 (2016).
[28] B. J. Crielaard *et al.*, Angew. Chem. **124**, 7366 (2012).
[29] E. Bardez *et al.*, J. Phys. Chem. B **101**, 7786 (1997).
[30] H. Zhang *et al.*, Org. Lett. **7**, 4217 (2005).
[31] H.-J. Butt *et al.*, Curr. Opin. Colloid Interface Sci. **59**, 101574 (2022).
[32] J. H. Snoeijer and B. Andreotti, Annu. Rev. Fluid. Mech. **45**, 269 (2013).
[33] T. D. Blake, J. Colloid Interface Sci. **299**, 1 (2006).
[34] S.-I. Lee and D.-J. Jang, J. Phys. Chem. **99**, 7537 (1995).
[35] A. Arce *et al.*, Phys. Chem. Chem. Phys. **6**, 103–108 (2004).
[36] P. P. Roussis, J. Membr. Sci. **15**, 141 (1983).
[37] A. S. Michaels and O. Morelos, Ind. Eng. Chem. **47**, 1801 (1955).